

Aerodynamic and Structural Optimisation of Maritime Patrol Radar System Radome using Evolutionary Algorithms

M.R. Shankar^{#,*}, A.C. Niranjappa[#] and B. Dattaguru[@]

[#]DRDO-Centre for Airborne Systems, Bengaluru - 560 037, India

[@]International Institute for Aerospace Engineering & Management, Jain University, Bengaluru - 562 112, India

^{*}E-mail: mrsankar@cabs.drdo.in

ABSTRACT

Airborne early warning systems are deployed for collecting surveillance information on airborne enemy targets in real-time. The Maritime Patrol Radar system is used for surveillance of sea surface for various types of ships and low flying aircraft. Radio Detection And Ranging system, or RADAR, in short, is an Electromagnetic sensor integrated on such airborne platforms. An antenna of this radar system is generally mounted under the belly of the aircraft and protected by a cover called a radome. This radome is installed to protect the radar antenna from environmental disturbances. Due to the installation of the radome, increased drag is experienced by aircraft during its flight due to resistance to the flow of the oncoming air. Radome design is a multidisciplinary effort involving structural, aerodynamics, and electromagnetic disciplines. In this study, the multi-disciplinary design of the maritime patrol aircraft radome for optimality in terms of structural strength and aerodynamic performance is carried out by integrating both disciplinary analyses on an optimisation software platform. The utopia point in terms of these two disciplines is found.

Keywords: MDO; Radomes; Aero-structural; A-sandwich; Pareto-front

NOMENCLATURE

AEW	Airborne Early Warning
BSE	Bore Sight Error
CEM	Computational Electro Magnetics
DOE	Design of Experiments
EM	Electro Magnetic
GA	Genetic Algorithm
GFRP	Glass Fibre Reinforced Plastic
MDO	Multidisciplinary Design Optimisation
MOGA	Modified Genetic Algorithm
MPR	Maritime Patrol Radar
NSGA	Non Sorting Genetic Algorithm
RADAR	RADio Detection And Ranging
TL	Transmission Loss
x, y, z	directions, coordinates
X, Y, Z	Forces in x, y, z directions

1. INTRODUCTION

MPR system is an airborne system deployed for airborne surveillance of the sea surface targets for getting location information of moving targets like ships, speed boats, etc., and also low flying enemy aircraft which could be potentially hostile. In this system, an Electro-Magnetic (EM) sensor called RADAR is mounted to detect these targets to provide early information to the operator. The radar consists of an antenna, transmission system, data processing system, etc.

As part of the MPR system, an antenna is installed below the fuselage to transmit/receive EM signals and covered with a radome. The cover to protect the antenna from the environmental effects like rain, ice, winds, dust, saline environment, etc., is called radome and it needs to be electromagnetically transparent to allow transmission of EM signals. In this paper, a multi-objective multi-disciplinary optimisation study is attempted for arriving at the configuration (shape, size, and thickness) of this radome by integrating aerodynamic and structural disciplines and modelling their interactions.

2. REVIEW OF LITERATURE

A study was undertaken by the authors for optimisation of the aerodynamic aspects of maritime radome in which the optimum point in terms of the drag of radome was evaluated¹. An extension of this optimisation considering structural and aerodynamics simultaneously is presented in this paper.

Radome protects the antenna which is housed inside but has to offer the least resistance to electromagnetic signals transmitted and at the same time structurally strong enough to withstand air loads and other environmental effects².

Kozakoff³ has explained various types of wall constructions for airborne radomes and their effect on EM transmission. It is brought out that the thin-walled or monolithic radomes are not found commonly in aircraft or missile applications since they cannot withstand the structural stresses. Sandwich radomes (A-sandwich or multilayer) are structurally strong and have wideband characteristics. However, more than five layers cause higher insertion loss or BSE.

Airborne radomes find different applications like fighter aircraft, missiles, transport aircraft, etc. However, in all of these cases, the underlying requirement is that they should withstand impact loads, pressure due to airflow, thermal conditions, etc. Important characteristics of radomes are high strength and stiffness, low weight, high radar transparency at selected EM frequency according to Manfred,⁴ et al. It was brought out that the radome design is a multi-disciplinary synergistic effort of structural mechanics, drop impact, radar optical behavior, and systems integration.

The design steps for ground surveillance radar on a transport aircraft were brought out by Pulvirenti,⁵ et al. The electromagnetic analysis, selection of materials for such radomes, structural analysis for air loads, and bird strike are elaborated. The size of the radome is limited by aircraft size. A bigger radome allows a bigger antenna to be accommodated resulting in lower BSE. The radome is analysed for air loads of sideslip conditions, water spray loads, rapid decompression, and bird strike. This study has dealt with a similar radome for which present optimisation is attempted. Although in this paper in literature, it was remarked that radome design is multi-disciplinary, such analysis was not carried out.

Kim⁶ has reviewed the role of CFD in aerodynamic optimisation for high fidelity analyses. It is proposed the use of GA with Kriging and Response Surface Modelling (RSM) for high fidelity models ensures global optimisation without getting trapped in local optimality. An air intake design by optimizing total pressure recovery is highlighted as a design case.

Deng⁷ *et al.* concentrated on the multi-disciplinary approach required for designing an airborne composite radar considering the EM and Structural aspects. Since the presence of radome can degrade the performance of the radar antenna, it is necessary to minimize two important EM parameters of radome namely BSE and TL. Besides, radome has to withstand the air-load and other environmental effects. Structural aspects considered are material failure (Tsai Wu index and maximum stress), deformation, and stability. Multi-island GA is used to optimize twin objectives of BSE and TL with constraints on material failure and structural stability.

Baker⁸ et al. brought out that unlike other aerospace structures, the design of radome involves considerations other than structural performance and it's a coupled problem of EM and structural requirements. In this study, aero-thermodynamic, structural, and EM aspects are integrated to perform a multi-disciplinary optimisation of a hypersonic vehicle radome. Various baseline geometries of Secant Ogive radome are stored in a library and called to perform linear structural analysis with inputs of pressure and temperature mapping from the flow and thermal analysis modules. Drag and transmission loss are taken as two objectives for minimisation in weighted optimisation.

Tang⁹ et al. provided a list of techniques used in EM analysis of radomes. The paper also brings out that the structural and EM characteristics are to be simultaneously considered in radome design in contrast to conventional design where these are considered in sequence with EM design first and structural aspects later. The thickness of each layer of the sandwich radome is taken as a design variable and with the

FEM model, both the structural and EM analysis is carried out. Transmission efficiency is maximised and with a maximum of failure-indices are ensured to be less than maximum allowed stress.

Xu¹⁰ has studied optimisation with Particle Swarm Optimisation techniques where the weighted sum of BSE, transmission loss, and variance of radome thickness is taken as the objective function. Thicknesses of various layers are design variables. 3D ray-tracing technique is used for electromagnetic analysis. It is also brought out that the streamlined shape of the radome results in the degraded performance of the antenna. It was concluded that with properly varying thickness, the efficiency of the radome can be improved.

Deng¹¹ et al attempted a multidisciplinary optimisation of A-sandwich radome with multi-island GA. Here the mechanical response (Tsai-Wu index) is taken as a constraint and the power transmission coefficient is maximised. Side constraints are applied on core and skin thickness of radome, frequency transmitted, and scan angles. Constant pressure is applied to the radome to find its mechanical response.

The thickness of the radome is a very important parameter in the design which holds the key to the transmission efficiency of the radome as well as its strength properties. Radomes are categorised based on the thickness as either thin or multiple one-half wavelengths. Kyung-Won Lee¹² et. al. explained that thin radome cannot meet the strength requirements and multiple one-half wavelength thickness radomes are very heavy in a monolithic structure.

3. AIRBORNE RADOMES

Airborne radome covering MPR antenna is generally oblong in shape and mounted on the centreline of the fuselage in the belly. This radome is symmetric about the longitudinal axis of the aircraft. A very important requirement of any airborne radome is that it should be as light as possible. At the same time, it should have the least drag and offer the least resistance to the EM signals being transmitted and received by the radar antenna. It should also withstand various structural and air loads it will experience in flight. These loads could be due to the air pressure, inertia loads, bird impact, and other loads during, taxiing, take-off, and landing.

Airborne radomes are classified mainly based on the type of construction and thickness. Thin-walled radomes are monolithic but are not generally suitable for airborne applications as they cannot meet structural requirements although they have excellent EM properties. Sandwich radomes are generally of A-sandwich or C-sandwich type and could be several half-wavelengths thick. They are broadband and have good structural properties as well.

4. RADOME DESIGN – MULTIDISCIPLINARY EFFORT

4.1 Overview

Radome design involves aerodynamic, structural, and electromagnetic disciplines among others and hence is a multidisciplinary effort. In this study, the interaction of aerodynamics and structures in the radome design are considered. The strength of the radome is dependent on the

material, cross-section, and geometry and the weight of the radome also depends on these. Since radome is installed externally it creates drag which can impact aircraft speed and hence range. As radome is a necessity, it is imperative that the effect of its installation, i.e., drag and weight need to be minimised. The design requirements for each of these disciplines could be contradictory in nature. Important design parameters in radome design are its geometry (length, width, height), cross-section properties, type of materials, and type of construction (monolithic or sandwich).

4.2 Aerodynamic Aspects

Any structure installed externally on the fuselage introduces resistance to airflow and hence additional drag. This drag is the sum of form drag (or pressure drag) and skin friction drag. Pressure drag depends on the form of radome and skin friction drag depends on the wetted area. Radomes are to be streamlined to minimize this drag. Due to the flow around the radome, air pressure acts on the radome. Pressure distribution due to airflow is an input for the structural design of radome. CFD analysis is carried out to estimate the drag due to the airflow and pressure distribution on the radome. Aerodynamic aspects and methods to evaluate drag and pressure distribution are discussed in a previous study by the authors¹.

4.3 Structural Aspects

Airborne radomes are generally made up of sandwich construction. Types of sandwich construction are illustrated in Fig 1. A sandwich is a composite structure that has a combination of FRP laminates (also called skin) and core. A laminate is an assemblage of continuous fibers embedded in a homogeneous matrix (resin). Glass, Carbon, and Aramid are some of the fibers generally used in composites. Honeycomb and Foam are some types of core materials.

Radomes should not be electrically conductive as they have to be electromagnetically transparent and hence materials used for radomes have to be non-conductive or polymeric. Two main types of sandwich used for radome are A-sandwich and C-sandwich. A-sandwich is preferred for radome because the transmission losses are less compared to C-sandwich although the latter is structurally stronger. In the current study, electromagnetically transparent polymeric A-sandwich radome is considered. GFRP and Aramid honeycomb are chosen as materials for skin and core respectively.

Pressure loading is one of the important aspects MPR radome has to withstand. Linear static analysis using FEM is to be carried out to evaluate if the radome design is capable of

withstanding the pressure loading. Since this is a polymeric composite sandwich radome, the Tsai-Wu criterion is used for checking this compliance. Any airborne store or item installed on the aircraft has to have as low as possible (minimum) weight.

5. MULTI-DISCIPLINARY MULTI-OBJECTIVE OPTIMISATION

5.1 Problem statement

Optimisation problem statement (Multi-disciplinary and Multi-objective) can be stated as follows

$$\text{Minimise } F(J_1(x), J_2(x)) \quad (1)$$

$$\text{subject to } Tsai - Wu_Index < 1.0 \quad (2)$$

$$\text{and } a \leq x \leq b \quad (3)$$

where $J_1(x)$ is Drag due to radome, $J_2(x)$ is Weight of the radome and x is a vector of design variables. Aerodynamic and structural optimisation is carried out for a chosen operational point of aircraft, i.e., for the aircraft flying at 0.4 Mach (137m/s) airspeed and 2438m (8000ft) altitude.

5.2 Design Objectives and Constraints

Drag (J_1) due to the airflow is the first design objective. Two main components of drag are form or pressure drag and parasite drag. The former is due to the blockage any shape offers to flow and the latter is dependent on the surface area wetted by the airflow. Streamlined shapes offer less form drag and more parasite drag due to large wetted area. On the other hand, bluff bodies have a lower surface area and hence have lower parasite drag but due to higher blockage, they offer higher form drag. The drag hence is a compromise in terms of length and bluntness of the shape.

Weight (J_2) of the radome is the second design objective. The weight of sandwich radome is dependent on the surface area, the number of laminae in the inner and outer skin, the thickness of the laminae (a constant here), and the thickness of the core. Weight of radome can be calculated with Eqn 4 given below

$$J_2 = SA_R * [(N_L * T_L * \rho_L) + (T_C * \rho_C)] \quad (4)$$

where SA_R is radome surface area, N_L is the number of laminae in the inner and outer skin, T is the thickness, ρ is the density, subscript L denotes Lamina, and subscript C denotes Core. The only design constraint is the Tsai-Wu Index (Eqn 5) of the radome under pressure loading, which should be less than 1.0. Apart from this design constraint, the lower and upper limits (a and b) of each design variable impose side constraints

$$F_1\sigma_1 + F_2\sigma_2 + 2F_{12}\sigma_1\sigma_2 + F_{11}\sigma_1^2 + F_{22}\sigma_2^2 + F_6\tau_{12} + F_{66}\sigma_6^2 \quad (5)$$

where F 's are constants calculated from material properties

5.3 Design Variables

In Fig. 2, points 1 to 11 are the control points that determine the cross-section of the radome under study. Point 0 is fixed at 0,0 (origin) and point 12 is fixed at L,0 where L is the length of the radome. Point 11 and Point 12 have the same 'x' value i.e., length of the radome. All the x coordinates (i.e., the horizontal distance from point 0) are varied as a percentage of total length "L". For example, if the radome length is 3.0 m, the 'x' coordinates of point 2 are varied from 20% to 25% of 3.0 m (0.6 to 0.75 m).

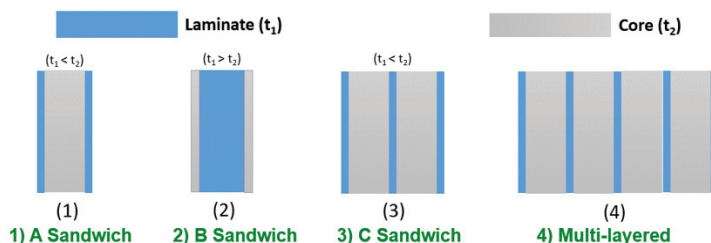


Figure 1. Types of Sandwich Construction.

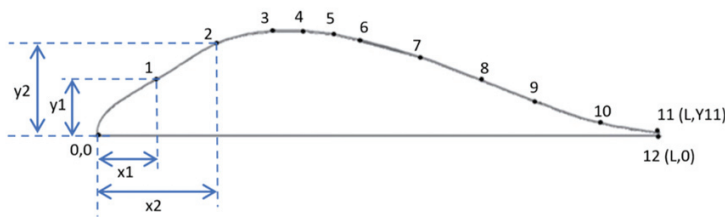


Figure 2. Radome 2D profile.

Variation in ‘x’ for each point is taken as 5% of length except for control points 9 and 10.

The coordinates (x and y) of control points (Points 1 to 11) in Fig. 2 are design variables¹. Hence by varying these coordinates, different cross-sections of the radome can be obtained. Additional design variables introduced for structural analysis are A-sandwich properties as given in Table 1. Ply angles of each lamina are set according to the number of laminae in outer and inner skins. Each lamina is assigned a ply angle i.e. first lamina ply angle is set to ‘0°’, 2nd lamina ply angle is set to ‘+45°’, 3rd lamina ply angle is set to ‘-45°’, and the fourth and last lamina is set to ‘90°’. For example, if the number of laminae in inner skin is set to 2, the thickness of 2nd and 3rd lamina is set to “0”. Lamina with “0” thickness does not participate in the analysis and the software (ANSYS ACP module) treats them as if they are absent. Hence the first and fourth lamina with ply angle ‘0°’ and ‘90°’ participate in the analysis. In the same way, the ply angles in outer skin laminae are also varied. When the laminae are 4 in both the skins this is known as quasi-isotropic layup (0°/±45°/90°).

Table 1. Design variables – Radome profile

Variable Description	Design Variable	Unit	Initial value	Lower bound	Upper bound	Step Size
Location 1 Length	x1	%**	0.12	0.10	0.15	0.0025
Location 2 Length	x2	%	0.22	0.20	0.25	0.0025
Location 3 Length	x3	%	0.32	0.30	0.35	0.0025
Location 4 Length	x4	%	0.42	0.40	0.45	0.0025
Location 5 Length	x5	%	0.52	0.50	0.55	0.0025
Location 6 Length	x6	%	0.62	0.60	0.65	0.0025
Location 7 Length	x7	%	0.72	0.70	0.75	0.0025
Location 8 Length	x8	%	0.82	0.80	0.85	0.0025
Location 9 Length	x9	%	0.92	0.90	0.94	0.001
Location 10 Length	x10	%	0.97	0.96	0.98	0.001
Location 1 Height	y1	m	0.2	0.17	0.25	0.005
Location 2 Height	y2	m	0.275	0.25	0.3	0.005
Location 3 Height	y3	m	0.325	0.30	0.35	0.005
Location 4 Height	y4	m	0.30	0.25	0.35	0.005
Location 5 Height	y5	m	0.25	0.20	0.30	0.005
Location 6 Height	y6	m	0.20	0.15	0.25	0.005
Location 7 Height	y7	m	0.20	0.15	0.25	0.005
Location 8 Height	y8	m	0.175	0.15	0.20	0.005
Location 9 Height	y9	m	0.125	0.10	0.15	0.005
Location 10 Height	y10	m	0.055	0.01	0.1	0.005
Location 11 Height	y11	m	0.029	0.008	0.05	0.005
Layers in outer skin	N _o	No	3	2	4	1
Layers in inner skin	N _i	No	3	2	4	1
Core thickness	T _c	mm	3	3	5	0.5

*all dimensions are in meters** as a percentage of current iteration length (L)

5.4 Aerodynamic Analysis

The process of aerodynamic analysis of the previous work¹ is used in this study also. The optimised radome had a drag value of 33N for a flow velocity of 103m/s and 2438m (8000ft). This could be due to the difference in the flow conditions and the number of optimisation iterations (700 in the earlier study). ANSYS Fluent[®] software was used to carry out CFD analysis for finding out the drag for a given profile by modifying an adaptive mesh which is refined as the profile of radome is changed. ANSYS workbench is programmed to re-adjust the CFD mesh based on the geometry and mesh parameters. CFD analysis is used to arrive at the pressure contour that needs to be imposed on the radome for structural analysis. Drag (J1) is calculated by integrating the pressure values over the surface of the radome by the software and provided as an output parameter.

5.5 Structural Analysis

Structural analysis is carried out using ANSYS[®] software. The radome is modelled with four layers of laminae (GFRP) on either side with a central core (Honeycomb). Material properties assigned to laminae and core are given in Table 2.

Default values in ANSYS ACP module are used for the analysis. For the initial geometry, a convergence study is carried out and after 8 iterations for stress and displacement convergence, it was found that a default mesh size of 10mm is appropriate. The surface is meshed with an automatic meshing algorithm in ANSYS Workbench with quad dominated (shell) elements of a default element size of 10mm. This quad element has four corner nodes and each node has six degrees of freedom (three translations and three rotations). A typical FEM mesh is shown in Fig. 3. This mesh is adaptive and it is refined every time the size & shape of the radome is changed. The edge of the radome which is attached to the aircraft is fully constrained. Depending on the number of layers in outer and inner laminates, the laminae are disabled in ANSYS ACP module as explained in paragraph 5.3 i.e., they do not participate in structural analysis. The thickness of each lamina is constant at 0.25mm. The pressure load from the CFD analysis is imposed on the surface of the radome.

6. OPTIMISATION PROCESS

The multi-objective optimisation was carried out with two algorithms implemented in modeFRONTIER[®] software, namely *MOGA-II* and *PiLOPT*. The optimisation process is depicted in the block diagram shown in Fig. 4. To start the optimisation process, an initial population is defined (for MOGA-II) or an initial design (for PiLOPT) is defined in step 1. Geometry details of the initial design are sent to CFD software to create the mesh and run the solver to estimate drag (J₁) and the pressure contour (steps 2, 3 & 4). The same geometry is sent to FE software to create FE mesh. The edge of the radome connected to the aircraft is fully constrained. The pressure loads from CFD are imposed on the outer surface (steps 5 &

Table 2. Material properties

Properties of GFRP	Properties of Honeycomb
$\rho = 1850\text{kg/m}^3$	$\rho = 80\text{kg/m}^3$
$E_x = 35\text{GPa}; E_y = 9\text{GPa}$	$E_x = 0.6\text{MPa}; E_y = 0.6\text{MPa}$
$G_{xy} = 4.7\text{MPa}$	$G_{xy} = 0.6\text{MPa}$
$\nu_{xy} = 0.28$	$\nu_{xy} = 0.1$
$X_t = 780\text{MPa}; X_c = 480\text{MPa}$	$X_t = 0\text{MPa}; X_c = 0\text{MPa}$
$Y_t = 31\text{MPa}; Y_c = 100\text{MPa}$	$Y_t = 0\text{MPa}; Y_c = 0\text{MPa}$
$S_{xy} = 60\text{MPa}$	$S_{xy} = 0\text{MPa}$

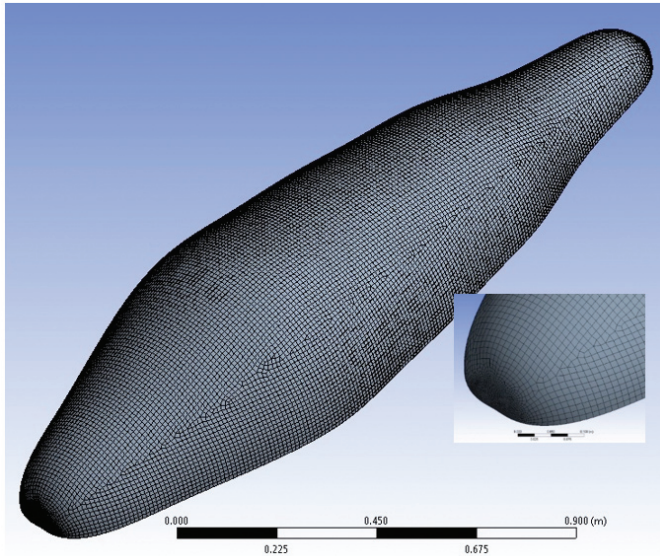


Figure 3. FEM model.

6). With linear static analysis, the Tsai-Wu index is calculated. Weight (J_2) of the radome is calculated based on the surface area of the radome, the number of laminae in the outer and inner skins, and the thickness of the core (step 7). Design objectives (J_1 and J_2) are read (step 8) and the design constraint (Tsai-Wu Index) is checked for compliance by the optimizer. The condition for stopping the process (step 9) is either completion of a certain number of iterations or if there is no improvement in designs in the *Pareto front*. The optimisation process is stopped if this condition is met. Otherwise, a new design is created (in PiLOPT) based on the values of objectives and constraints the process is repeated. In the MOGA-II, after one generation of designs is evaluated, the next-generation is created (step 10).

7. RESULTS AND DISCUSSION

7.1 MOGA-II Algorithm

An initial population of ten designs is generated using Latin-Hypercube sampling as the first generation of designs. Using the MOGA-II algorithm, 100 generations were created and analysed. The objective values of designs are plotted in Fig. 5. The designs in the Pareto front are marked with red diamonds. A closer view of the *Pareto front* (designs connected by the red line) is depicted in the inset figure. The Pareto front has fifteen radome designs.

The designs are non-dominated i.e., a reduction in one objective is accompanied by an increase in another objective in this front. In the *Pareto front*, a designer can find designs with varying preferences of objectives. For example, the

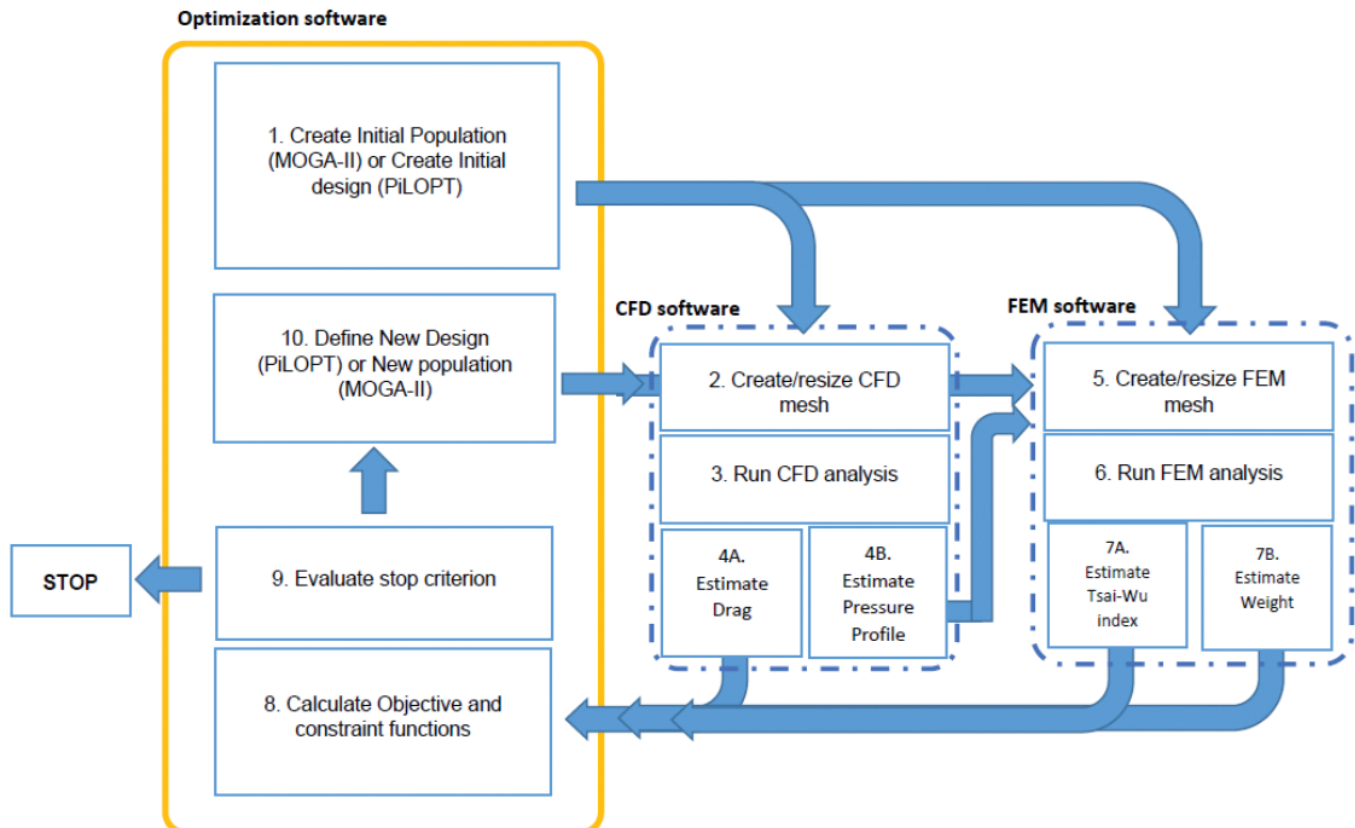


Figure 4. Optimisation Process Flow.

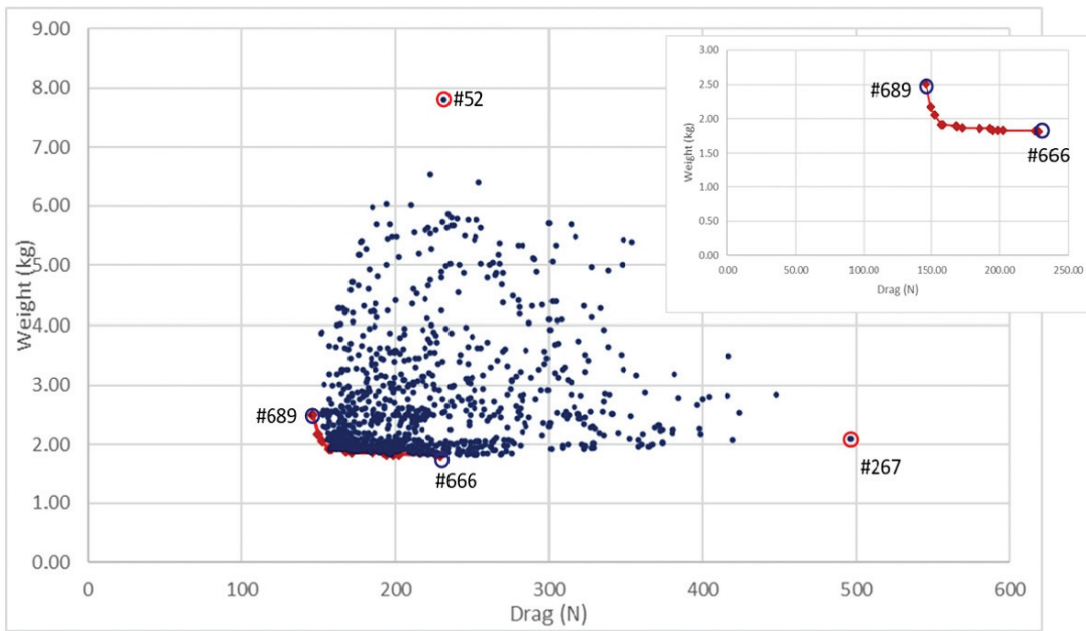


Figure 5. Designs with MOGA-II algorithm.

least drag design has 145.8N drag and 2.50kg weight. If we move on the Pareto front, the next design has 149.6N drag (an increase of 2.6%) and weighs 2.17kg (a decrease of 13%). Hence if the designer can compromise little on drag, there is an improvement in weight. Analysing more generations might define the Pareto front better. The point in design space where both drag and weight are minima (*Utopia point*) is at (145.8N, 1.816Kg) with MOGA-II algorithm. The variation in drag of the designs explored is from 145 to 496N. The variation in weight is from 1.82 to 7.8 kg. Profiles of different radomes are compared in Fig. 6, which are some of the best and worst designs. Case #689 and #666 are in the Pareto front and have the least drag and least weight in that order. Of all the designs evaluated, Case #267 and case #52 are worst in terms of drag and weight in that order. Case #52, one of the longest radome and heaviest, has 4 laminae in inner and outer skins and a core thickness of 3.5mm.

The weight is a linear function of the surface area, the number of layers in the outer skin, the number of layers in the inner skin, and the core thickness. Case #267 is having the highest drag because of its wavy shape which increases the surface area as well as pressure drag. The drag is a function of surface area and the kinkiness in the profile and both of which have increased it.

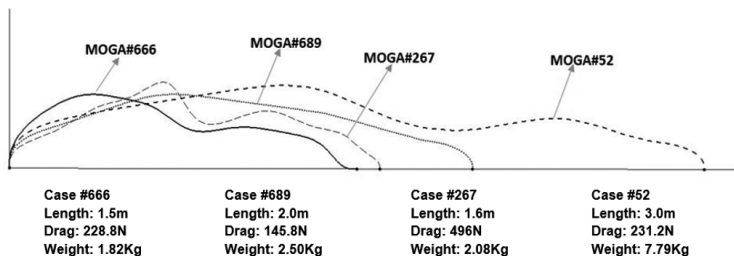


Figure 6. Radome profiles - MOGA-II algorithm.

7.2 PiLOPT Algorithm

More than 1200 computer runs were carried out with this algorithm and the objective values of designs are plotted in Fig 7. A closer view of the Pareto front is inset in the figure (designs connected by the red line). The designs in the Pareto front are marked with red diamond symbols. The *Pareto front* has forty-four radome designs.

The *Pareto front* here is better than the previous case. The point in design space where both drag and weight are minima (*Utopia point*) is at (146N, 1.589kg) with the PiLOPT algorithm. The variation in drag of the designs explored is from 146 to 785N. The variation in weight is from 1.58 to 8.33 kg. Profiles of different radomes are compared in Fig 8, which are some of the best and worst designs. Case #1176 and #1127 are in the *Pareto front* and have the least drag and least weight in that order. Of all the design cases analysed, Case #92 and case #12 are worst in terms of drag and weight in that order. Even though #92 is of the same length as #1127 (1.5m), it has more drag due to its highly wavy shape which increases pressure drag. Case #12 has the highest weight even though it is streamlined because it is the longest of all and has four layers of GFRP in outer and inner skin with a core thickness is 4mm.

More than half the designs evaluated in the PiLOPT are in 1.5m radome length, which indicates that the algorithm tries to evaluate more designs near or in the optimum zone. With MOGA-II algorithm, the generations evolve and move towards optimum designs steadily. Longer radome designs are less as these are found to be less optimal.

With MOGA II algorithm, the generations are spread out in various lengths to find the Pareto front, although the number of design points in the Pareto front is comparatively less than PiLOPT. In contrast, the PiLOPT algorithm seems to evaluate the design space near the optimum, however able to get a greater number of designs in the Pareto front.

Comparison of best designs (lowest drag and weight)

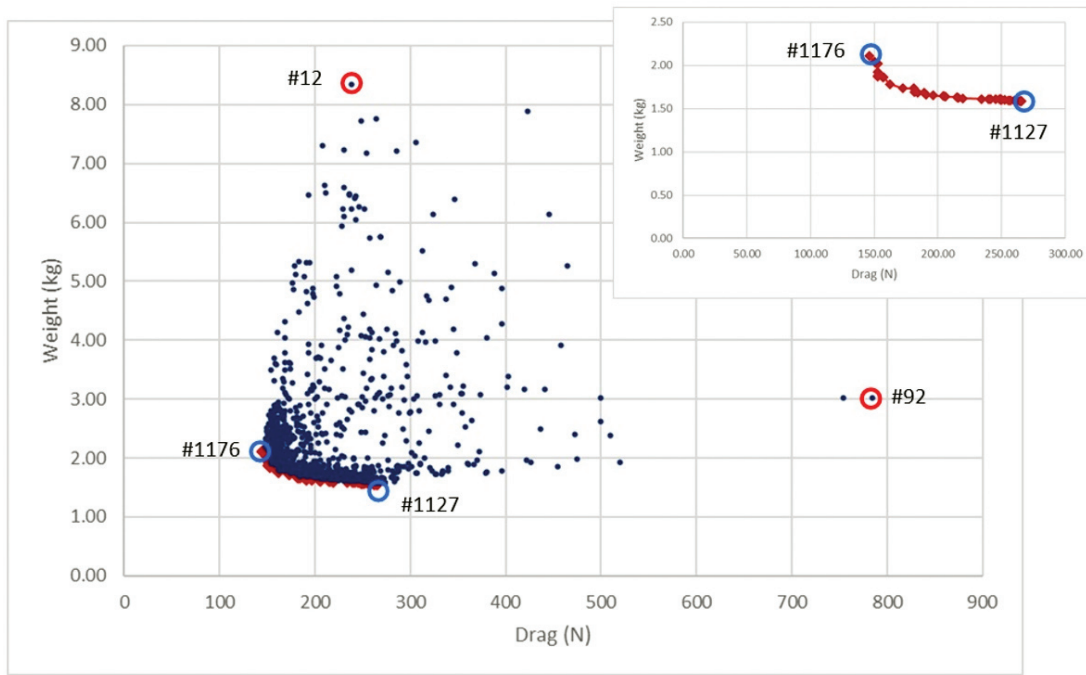


Figure 7. Designs with PiLOPT algorithm.

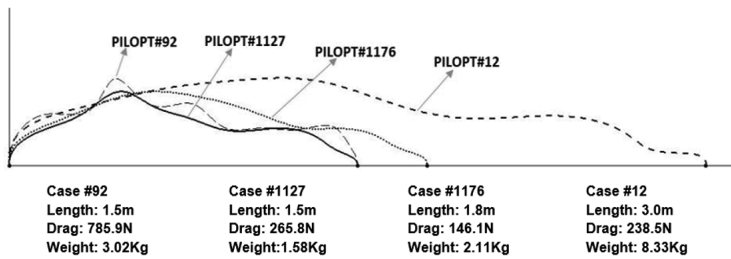


Figure 8. Radome profiles - PiLOPT algorithm.

Table 3. Comparison of best designs

	PiLOPT algorithm		MOGA II algorithm	
	Lowest Drag	Lowest Weight	Lowest Drag	Lowest Weight
Run ID	#1176	#1127	#689	#666
Drag (N)	146.1	265.8	145.8	228.9
Weight (kg)	2.113	1.589	2.504	1.816
Length of radome (m)	1.8	1.5	2.0	1.5
<i>UtopiaPoint</i> (Drag, Weight)	146.1N, 1.588Kg		145.8N, 1.816Kg	

on the Pareto front from both runs are given in Table 3. The variation in drag is from 145 to 785N. The variation in weight is 1.58 to 8.33 kg.

8. CONCLUSION

Multi-objective optimisation of the radome was performed using two algorithms namely PiLOPT and MOGA-II and the results were compared. It is found that both algorithms are close in estimating best designs, for the number of designs evaluated. The drag of the optimised radome of aerodynamic study is 33.5N, whereas, in the present study, the lowest value of drag is increased. This can be because the flow conditions

are different and due to combined aero-structural optimisation.

Utopia points estimated by both algorithms have similar drag values but differ in weight by 15%. *Utopia points* are designs with theoretical minimum and hence such design does not exist where both the objectives are simultaneously at their minimum.

The lowest drag designs have similar drag but have a weight variation of about 20%. In the lowest weight designs, variation in weight is 15% and variation in drag is 16%. The lowest weight designs have the same length of 1.5m. While with MOGA-II, a 2.0m long radome has lower drag compared to a 1.8m long radome with PiLOPT.

For a designer, if the drag of the radome is more important among the two objectives, the lowest drag design by either algorithm is acceptable. However, if the weight is the deciding factor, the lowest weight design by PiLOPT is a clear choice. In both cases, the designs are good starting points and higher fidelity analyses & corroboration by wind tunnel testing may be required for arriving at the actual values achievable.

Pareto front considering these two disciplines was discovered for one operating condition of the MPR system. PiLOPT algorithm provides less weight design compared to MOGA II whereas both algorithms give nearly the same value for lowest drag.

Aerodynamics optimisation can lead to an optimised streamlined shape of the radome, but without the consideration of structural design. A physical design of radome cannot be achieved in aerodynamic optimisation which is possible with aero-structural optimisation. However, the Electro-magnetic discipline needs to be integrated into the above framework to evaluate the combined effect of all three disciplines.

REFERENCES

1. Shankar, M. R.; Niranjana, A. C.; & Dattaguru, B. Aerodynamic optimization of airborne radome for maritime patrol radar. *Int. J. Engg. and Adv. Tech.*, 2020, **9**(3).
doi:10.35940/ijeat.B3422.029320
2. Military specification: General Specifications for Radomes, MIL-R-7705 B, 1975, available at http://everyspec.com/MIL-SPECS/MIL-SPECS-MIL-R/MIL-R-7705B_24492/
3. Natter, M.; Schroder H.-W.; & Scharafer, W. Radome technology, *In Proceedings of 16th Int. Counc. Aeronaut. Sci.*, 1988, 2, 1634-1640
4. Kozakoff, D. J. Dielectric wall constructions, *In Analysis of radome-enclosed antennas*, Artech House, 685, Canton Street, Norwood, MA 02062 USA, 2010, pp 88-102.
5. Pulvirenti, G.; Tromboni, P.D.; Marchetti, M.; Delogu, A.; Maccapani, A. & Aricò, R. Surveillance system airborne composite radome design., *In Proc. Int. Conf. Fract*, 2005, 1, 233-238.
6. Chongam, K. Computational elements for high-fidelity aerodynamic analysis and design optimisation. *Def. Sci. J.*, 2010, **60**(6), 628-638.
doi: 10.14429/dsj.60.581
7. Deng, J.; Zhou. G.; & Qiao. Y. Multidisciplinary design optimization of sandwich-structured radomes, *In Proc. Inst. Mech. Eng., Part C, J. Mech. Eng. Sci.*, **233**(1),2019,179-189.
doi:10.1177/0954406218757268.
8. Baker, M. L.; Roughen, K. M.; Moylan, B. E.; & Russell, G. W. Structural optimization with probabilistic fracture constraints in the multidisciplinary radome optimization system, AIAA-2007-2311, *In Proc. 48th AIAA/ASME/SAE Struct., Struct. Dyn., Mater. Conf.*, 2007, 7.
doi:10.2414/6.2007-2311.
9. Tang, X.; Zhang, W.; & Zhu. J. Multidisciplinary optimization of airborne radome using genetic algorithm In: Deng, H.; Wang, L.; Wang, F.L.; & Lei J. (eds) *Artificial Intelligence and Computational Intelligence. AICI 2009. Lecture Notes in Computer Science.*, 5855, Springer, 2009.
doi:10.1007/978-3-642-05253-8_17
10. Xu, W. Y. Thickness profile design of airborne radomes with thickness control, *In Proceedings Fifth Asia International Symposium on Mechatronics.*, 2015, 1-4, <https://digital-library.thiet.org/content/conferences/10.1049/cp.2015.1054>.
11. Deng, J.; & Zhou, G. A multi-disciplinary optimization design method for airborne radome, *In Proceedings of AIAA Modeling and Simulation Technologies Conference*, 2017.
doi:10.2514/6.2017-4336
12. Lee, K.; Chung, Y.; Hong, I. & Yook, J. An effective design procedure for A-sandwich radome, *In Proceedings of 2010 IEEE Antennas and Propagation Society International Symposium.*, 2010, 1-4.
doi:10.1109/APS.2010.5561702

ACKNOWLEDGEMENTS

Authors acknowledge permission given by Mr. M S Easwaran, Distinguished Scientist and Director, CABS for carrying out this study with the software and computing facility at CABS aircraft group. The support provided by colleagues in the Aircraft group, CABS is much appreciated.

CONTRIBUTORS

Mr M.R. Shankar is a PhD scholar at IIAEM, Jain (Deemed to be university), Bengaluru and Scientist F & Head Aircraft Division in Centre for Airborne Systems (DRDO), Bengaluru, India. He has more the 20 years of experience in aircraft structural modification & integration, new product development, structural design and optimisation. He carried out disciplinary modelling and integration, carried out the analysis and compiled results.

Dr A.C. Niranjana, Outstanding Scientist is Group Director for Aircraft Operations at Centre for Air Borne Systems (DRDO), Bengaluru, India. He is an expert in the field of Advanced Polymer Composites and specialised in the design and development of sandwich radomes for airborne applications. He has been working in the field of Aircraft Structural modifications, integration of Airborne surveillance mission systems and flight test R&D activities from the last 30 years. He guided principal author as internal guide in structural disciplinary modelling, interpretation of structural analysis of results.

Prof. B. Dattaguru retired as Chairman of Department of Aerospace Engineering, Indian Institute of Science, Bangalore and currently working as Professor at Jain (deemed-to-be-University). His fields of interest are Aerospace Structures and materials, Fracture and Computational mechanics. He published 207 papers in various journals and conference proceedings. He received several awards, notable among them being Rustom Choksi award for excellence in Engineering Research (IISc), Academic Excellence award (DRDO) and Padmashree (Govt. of India), ICCES – 2014 Lifetime Achievement at Changwon, Korea and APCAM Senior Scientist awards at Sydney. He guided principal author in validating the MDO frame work, interpretation of MDO results and presentation.